

# Towards the emerging source class of $\gamma$ -ray emitting colliding-wind binary systems

---

**K. Reitberger<sup>\*†‡</sup>, R. Kissmann, A. Reimer<sup>†</sup> and O. Reimer<sup>†</sup>**

*Institut für Astro- und Teilchenphysik and Institut für Theoretische Physik,  
Leopold-Franzens-Universität Innsbruck, A-6020 Innsbruck, Austria*

*E-mail: klaus.reitberger@uibk.ac.at*

Recently published results using seven years of *Fermi*-LAT data shed new light on the still puzzling source class of particle-accelerating colliding-wind binary (CWB) systems. While the claimed association of the system  $\gamma^2$  Velorum (WR 11) with a high-energy  $\gamma$ -ray source contrasts the exclusivity of  $\eta$  Carinae as the hitherto only detected  $\gamma$ -ray emitter of that sort, the low upper limits obtained for WR 140 strengthen the question why this system with all its similarities to the  $\gamma$ -ray bright  $\eta$  Carinae remains still unseen.

We use three-dimensional magneto-hydrodynamic modeling (MHD) to investigate the structure and conditions of the wind-collision region (WCR) in these three systems, including the important effect of radiative braking in the stellar winds. A transport equation is then solved throughout the computational domain to study the propagation of relativistic electrons and protons. The resulting distributions of particles are subsequently used to compute nonthermal photon emission components.

With the above procedure, we obtained first model results that can account for the weak detection of  $\gamma^2$  Velorum, the strong detection of  $\eta$  Carinae, and the non-detection of WR 140 in a similar computational setup.

*7th Fermi Symposium 2017  
15-20 October 2017  
Garmisch-Partenkirchen, Germany*

---

<sup>\*</sup>Speaker.

<sup>†</sup>on behalf of the *Fermi*-LAT collaboration

<sup>‡</sup>The *Fermi*-LAT Collaboration acknowledges support for LAT development, operation and data analysis from NASA and DOE (United States), CEA/Irfu and IN2P3/CNRS (France), ASI and INFN (Italy), MEXT, KEK, and JAXA (Japan), and the K.A. Wallenberg Foundation, the Swedish Research Council and the National Space Board (Sweden). Science analysis support in the operations phase from INAF (Italy) and CNES (France) is also gratefully acknowledged. This work performed in part under DOE Contract DE-AC02-76SF00515. The computational results presented have been achieved (in part) using the HPC infrastructure of the University of Innsbruck.

## 1. Introduction

Since the early days of *Fermi*-LAT observations researchers have been puzzled by the non-detection of certain massive star binary systems. Based on the predictions of analytical models, WR 147 and WR 140, two systems with colliding stellar winds of high momenta, have been frequently named as promising (strong) sources for high-energy  $\gamma$ -ray radiation in the pre-*Fermi* era [1, 2, 3]. They have not been detected, neither in a dedicated analysis of 2 years of Pass 7 data [4], nor in a more recent analysis of 7 years of Pass 8 data [5]. The non-detection of these sources becomes even more puzzling when we consider the detection of two other systems of massive stars with colliding-winds where the same physical processes are thought to occur:  $\eta$  Carinae and  $\gamma^2$  Velorum. For WR 140 an upper limit of  $F_{100\text{MeV}}^{100\text{GeV}} < 1.1 \times 10^{-9} \text{ph m}^{-2} \text{s}^{-1}$  [5] now contrasts the bright detection of  $\eta$  Car at  $F_{100\text{MeV}}^{100\text{GeV}} = 1.84 \pm 0.30 \times 10^{-7} \text{ph m}^{-2} \text{s}^{-1}$  [6]. Considering the similarity between these two systems in terms of period, eccentricity, stellar separation, or distance and the fact that WR 140 has an even higher total kinetic wind power than  $\eta$  Carinae, this stark contrast in high-energy  $\gamma$ -ray flux is quite a surprise.

Using advanced MHD modeling in conjunction with the solution of the transport equation of high-energy particles, we seek to identify a common property of the two  $\gamma$ -ray bright systems,  $\gamma^2$  Velorum and  $\eta$  Carinae, which distinguishes them from the  $\gamma$ -ray dark system of WR 140.

## 2. The model

The numerical modeling framework used in this study is identical with the one presented in detail in [7] and [8] – including the improvements and modifications discussed and described in [9] and [10]. We use a MHD code to model the threedimensional distribution of wind plasma density, velocity, temperature and magnetic field strength. At the same time a transport equation is iteratively solved for every grid cell and time step. This provides us with a threedimensional distribution of particle spectra for electrons and protons throughout the simulated volume. In a subsequent step, the modeled properties of the wind plasma and the particle spectra are used to compute components of nonthermal emission (via synchrotron, relativistic bremsstrahlung, inverse Compton emission, and neutral pion decay) including attenuation effects by photon-photon absorption in the dense stellar radiation fields.

## 3. Hydrodynamics

The modeled wind plasma density of the three CWBs under investigation for the orbital state of apastron – shown in Fig. 1 – reveals one common property of the two systems which are seen in high-energy  $\gamma$ -ray energies.  $\eta$  Carinae and  $\gamma^2$  Velorum both show maximum wind-plasma densities in the WCR higher than  $10^{16} \text{m}^{-3}$ . The respective value for WR 140 – the system which remains unseen in  $\gamma$  rays – is roughly 3 orders of magnitudes lower. The reason for the very high wind plasma densities in two of these three systems are the following:  $\gamma$  Velorum’s comparatively short period leads to low stellar separation and therefore low distances between the WCR and the stars. The winds collide long before reaching terminal velocity at a distance from the OB star where its wind density is still very high. In the case of  $\eta$  Carinae, stellar separation is high. However, the

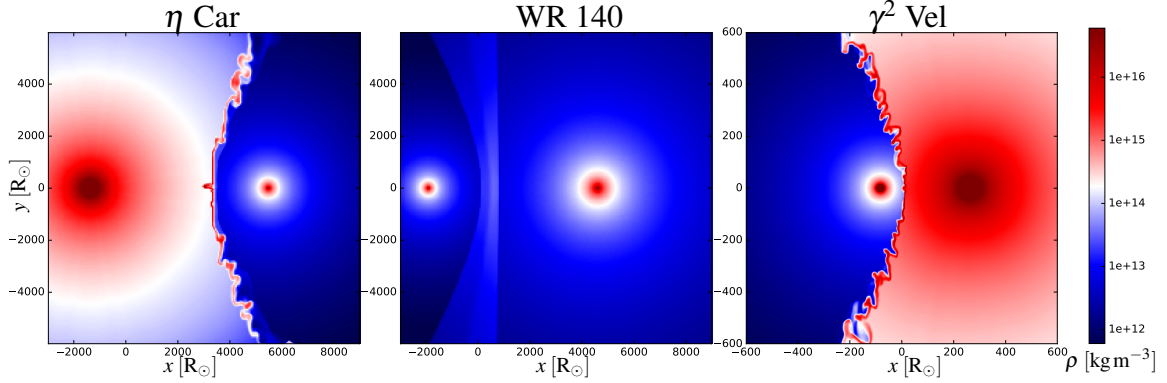


**Figure 1:** Density of wind plasma at apastron for  $\eta$  Carinae, WR 140, and  $\gamma^2$  Velorum. The star identified (and modeled) as W–R star are always on the right-hand side, the OB or LBV stars on the left-hand side. The computational domain of the plot on the left-hand side in the center is 12 000  $R_{\odot}$  wide. For the plot on the right-hand side it is merely 1200  $R_{\odot}$ .

unusual nature of the primary star – a Luminous Blue Variable with one of the highest mass-loss rates known in the Galaxy – leads to a very dense primary wind and therefore to high plasma density on the primary-side of the WCR. For WR 140, where we find more ordinary stellar parameters and large stellar separation, the plasma density in the WCR remains much lower.

#### 4. Particle spectra

The question whether the apparent contrast in wind plasma density relates to a similar contrast in the distribution of particles has to be answered in the negative. Although the implemented formula for particle injection at the shock front suggests a linear dependence on the wind plasma density, this would neglect the impact of loss rates (depending on stellar wind parameters), diffusion, the volume of the emission region, as well as different acceleration efficiencies. In WR 140, lower wind plasma density leads to lower loss rates by Coulomb losses and losses from nucleon-nucleon collision. At the same time higher wind velocities lead to more efficient particle acceleration. These effects suffice to diminish the increased particle acceleration due to higher plasma density. Figure 2 – showing proton densities at 1 MeV and 10 GeV – does not indicate a contrast comparable with the 3 orders of magnitude difference that has been found for the density. In terms of proton spectra – shown in Fig. 3 (left) – we find the maximum energies for  $\eta$  Carinae to be slightly higher. However, the amplitudes of the spectra are comparable for all three systems.

#### 5. Hadronic $\gamma$ -ray emission

Using the obtained particle spectra for the computation of  $\gamma$ -ray emission via the neutral pion decay channel we find the previously shown contrast in density to re-emerge in the obtained SEDs. As shown in Figure 3 (right), the neutral pion decay component of  $\eta$  Carinae lies significantly (up to 3 orders of magnitude) above the SED of WR 140. This follows from the formula implemented for the computation of pion spectra [12] which is proportional to the wind plasma density.

It has to be stressed that the simulation results for  $\eta$  Carinae and WR140 – as they are shown in Fig. 3 (right) – rely on exactly the same simulation procedure. All free parameters – including

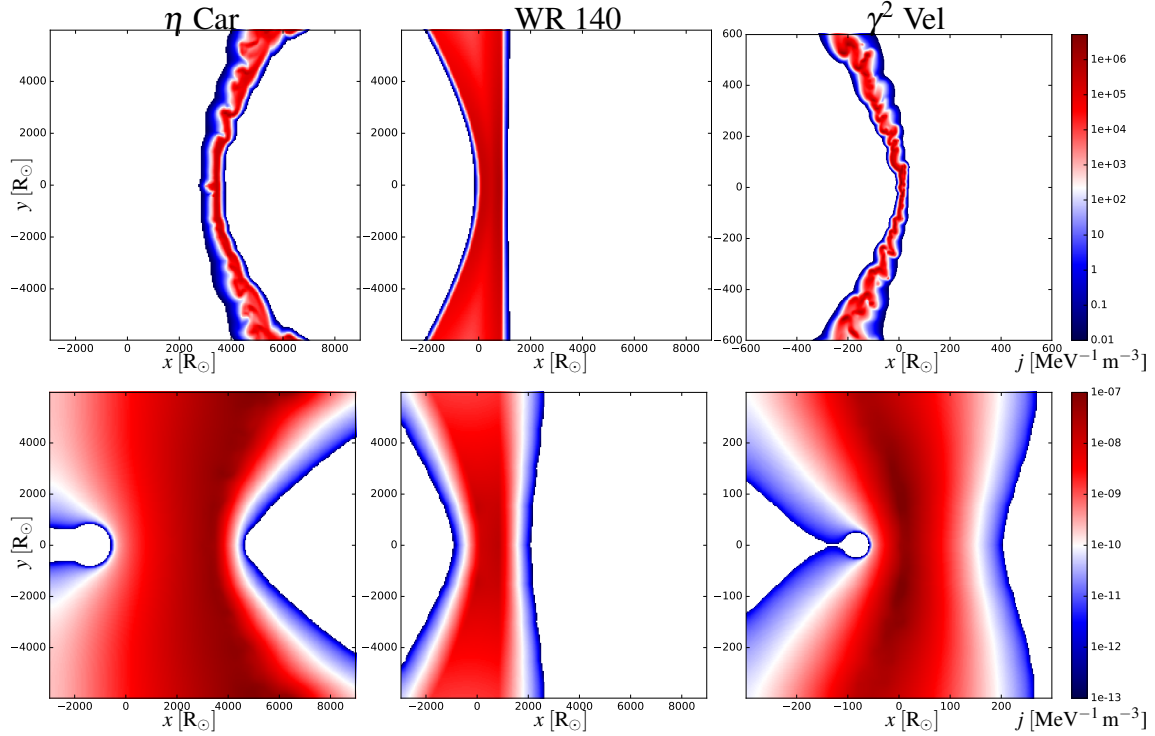


**Figure 2:** Protons at 1 MeV (top row) and at 10 GeV (bottom row) at apastron for  $\eta$  Carinae, WR 140, and  $\gamma^2$  Velorum. Same arrangement as in Fig. 1.

diffusion coefficient normalization and injection rate – are kept at the same values ( $\eta_p = 4 \times 10^{-3}$ ,  $D_0 = 10^{16} \text{m}^2 \text{s}^{-1}$ ). The only difference lies in the known stellar, stellar-wind and orbital parameters. Our simulations are thus able to reproduce the once puzzling discrepancy between the strong detection of  $\eta$  Carinae and the non-detection WR 140. The simulation results for the observed, but weak  $\gamma$ -ray source of  $\gamma^2$  Velorum lie in between and can also be brought into agreement with the measured data.

The peculiar double-peak structure of the neutral pion peak of  $\eta$  Carinae stems from the different conditions at the two shocks which form the boundary of the WCR.

## 6. Conclusion

The situation, in which one predicted source is detected and another one remains dark, poses a problem. To successfully resolve this problem, we need a model which at the same time accounts for the observed signal of one system and the non-detection of the other – without introducing any difference in method or any unwarranted shift in parameters between the two systems. This has been achieved by the present analysis. The contrast of maximum wind plasma density of more than three orders of magnitude in the WCR of WR 140 and  $\eta$  Carinae has been identified as the vital difference between these systems that ultimately results in their completely unlike  $\gamma$ -ray brightness.

The system of  $\gamma^2$  Velorum serves as an intermediary system where the relative proximity of the WCR and the stars results in high plasma densities in the WCR. This, together with the relatively low distance to Earth, leads to a weak but detectable  $\gamma$ -ray signal. Model predictions and observations are found to agree.

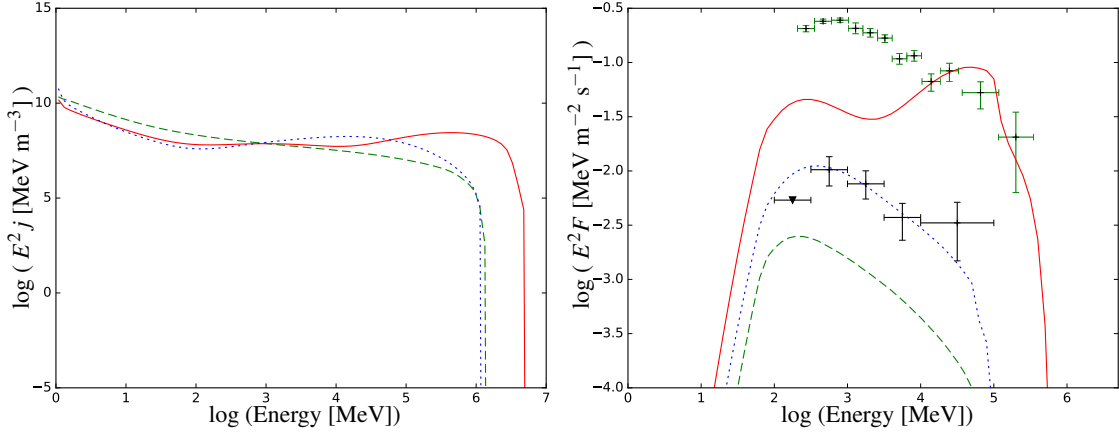


**Figure 3:** Left: number density of protons integrated over the computational domain. Right: The resulting SEDs for the neutral pion decay emission channel. Also shown are the *Fermi*-LAT data points determined for  $\gamma^2$  Velorum (black) [5] and for  $\eta$  Carinae (green) [11]. Both:  $\eta$  Carinae (red solid), WR 140 (dashed green),  $\gamma^2$  Velorum (blue dotted).

## 7. Outlook

The present analysis does not yet consider the full orbit of the three binary systems. Distortions of the WCR due to orbital motion are neglected. Simulations are currently being run which consider several orbits, thus taking us from the presented orbital snapshot to a multi-orbital analysis. Once we are able to make predictions on the expected orbital variability in the form of light curves, comparison with the newest available data [13] will put constraints on the range of parameters and the details of our method.

This study focuses on the hadronic emission component. It remains to be investigated, whether the low-energy ( $< 10$  GeV) part of the  $\eta$  Carinae spectrum can be attained by a leptonic component from inverse Compton decay. To this end, higher maximum electron energies have to be reached. The strong radiation field of the LBV star apparently excludes this possibility. However, if we consider an attenuation of the LBV's radiation on the far side of the WCR in the WR wind, higher electron energies will become possible in this region.

Applied to other candidates for particle-accelerating CWB systems (see catalogue by [14]), the presented simulation method can be used to make predictions about their future detectability in the high-energy  $\gamma$ -ray regime. It may pave the way towards the emerging source class of  $\gamma$ -ray emitting colliding-wind binary systems.

## 8. Questions during Discussion

D. Torres: *Do you also consider the contributions of secondary electrons produced in the pion decay on the total electron spectrum and the leptonic  $\gamma$ -ray emission components?*

Answer: No, not yet. (Remark: This is an excellent topic for a future Master student and might be addressed in the near future.)

M. Boettcher: *Newest H.E.S.S. results show a detection  $\eta$  Carinae beyond  $\sim 300$  GeV which is in contradiction to your model.*

Answer: On first glance, probably yes. It remains to be seen at what amplitude the detected flux is. (Remark: With the free parameter of the diffusion coefficient normalization we can in principle adjust the maximum energies attained by the protons and thus influence the high-energy cutoff of the  $\gamma$ -ray SED by neutral pion decay. It might well be, that agreement can be found between the new H.E.S.S. results and the prediction of our model by changing this parameter. )

## References

- [1] D. Eichler and V. Usov, *Particle acceleration and nonthermal radio emission in binaries of early-type stars*, *ApJ* **402** (Jan., 1993) 271–279.
- [2] P. Benaglia and G. E. Romero, *Gamma-ray emission from Wolf-Rayet binaries*, *A&A* **399** (Mar., 2003) 1121–1134, [arXiv:astro-ph/0205375].
- [3] A. Reimer, M. Pohl and O. Reimer, *Nonthermal High-Energy Emission from Colliding Winds of Massive Stars*, *ApJ* **644** (June, 2006) 1118–1144, [astro-ph/0510701].
- [4] M. Werner et al., *Fermi-LAT upper limits on gamma-ray emission from colliding wind binaries*, *A&A* **555** (July, 2013) A102, [1308.2573].
- [5] M. S. Pshirkov, *The Fermi-LAT view of the colliding wind binaries*, *MNRAS* **457** (Mar., 2016) L99–L102, [1510.03885].
- [6] F. Acero, M. Ackermann, M. Ajello, A. Albert, W. B. Atwood, M. Axelsson et al., *Fermi Large Area Telescope Third Source Catalog*, *ApJS* **218** (June, 2015) 23, [1501.02003].
- [7] K. Reitberger, R. Kissmann, A. Reimer, O. Reimer and G. Dubus, *High-energy Particle Transport in Three-dimensional Hydrodynamic Models of Colliding-wind Binaries*, *ApJ* **782** (Feb., 2014) 96, [1401.1323].
- [8] K. Reitberger, R. Kissmann, A. Reimer and O. Reimer, *Simulating Three-dimensional Nonthermal High-energy Photon Emission in Colliding-wind Binaries*, *ApJ* **789** (July, 2014) 87, [1405.6868].
- [9] R. Kissmann, K. Reitberger, O. Reimer, A. Reimer and E. Grimaldo, *Colliding-wind Binaries with Strong Magnetic Fields*, *ApJ* **831** (Dec., 2016) 121, [1609.01130].
- [10] K. Reitberger, R. Kissmann, A. Reimer and O. Reimer, *MHD Models of Gamma-ray Emission in WR 11*, in *American Institute of Physics Conference Series*, vol. 1792, Jan., 2017, DOI.
- [11] K. Reitberger, A. Reimer, O. Reimer and H. Takahashi, *The first full orbit of  $\eta$  Carinae seen by Fermi*, *A&A* **577** (May, 2015) A100, [1503.07637].
- [12] S. R. Kelner, F. A. Aharonian and V. V. Bugayov, *Energy spectra of gamma rays, electrons, and neutrinos produced at proton-proton interactions in the very high energy regime*, *Phys. Rev. D* **74** (Aug., 2006) 034018, [astro-ph/0606058].
- [13] M. Balbo and R. Walter, *Fermi acceleration along the orbit of  $\eta$  Carinae*, *A&A* **603** (July, 2017) A111, [1705.02706].
- [14] M. De Becker and F. Raucq, *Catalogue of particle-accelerating colliding-wind binaries*, *A&A* **558** (Oct., 2013) A28, [1308.3149].